Published in final edited form as:
J Neuroimaging. 2018 January ; 28(1): 86–94. doi:10.1111/jon.12486.

Cerebral white matter maturation patterns in preterm infants: an MRI T2 relaxation anisotropy and diffusion tensor imaging study

Michael J. Knight, PhD[1], **Adam Smith-Collins, PhD**[2,3], **Sarah Newell, MD**[3], **Mark Denbow**[3], and **Risto A. Kauppinen, MD PhD**[1,2]

[1]School of Experimental Psychology, University of Bristol, United Kingdom

[2]Clinical Research and Imaging Centre, University of Bristol, United Kingdom

[3]Fetal Medicine Unit, St Michael's Hospital, University Hospitals Bristol NHS Foundation Trust, United Kingdom

Abstract

Background and Purpose—Preterm birth is associated with worse neurodevelopmental outcome, but brain maturation in preterm infants is poorly characterised with standard methods. We evaluated white matter (WM) of infant brains at term-equivalent age, as a function of gestational age at birth, using multi-modal MRI.

Methods—Infants born very pre-term (< 32 weeks gestation) and late pre-term (33-36 weeks gestation) were scanned at 3T at term-equivalent age using diffusion tensor imaging (DTI) and T2 relaxometry. MRI data were analysed using tract-based spatial statistics, and anisotropy of T2 relaxation was also determined. Principal component analysis and linear discriminant analysis were applied to seek the variables best distinguishing very pre-term and late pre-term groups.

Results—Across widespread regions of WM, T2 is longer in very pre-term infants than in late pre-term ones. These effects are more prevalent in regions of WM which myelinate earlier and faster. Similar effects are obtained from DTI, showing that fractional anisotropy (FA) is lower and radial diffusivity higher in the very pre-term group, with a bias towards earlier myelinating regions. Discriminant analysis shows high sensitivity and specificity of combined T2 relaxometry and DTI for the detection of a distinct WM development pathway in very preterm infants. T2 relaxation is anisotropic, depending on the angle between WM fibre and magnetic field, and this effect is modulated by FA.

Conclusions—Combined T2 relaxometry and DTI characterises specific patterns of retarded WM maturation, at term equivalent age, in infants born very pre-term relative to late pre-term.

Keywords

MRI; preterm birth; diffusion tensor imaging; T2 relaxometry; white matter

Corresponding author: Professor Risto Kauppinen, School of Experimental Psychology, University of Bristol, 12a Priory Road, Bristol BS8 1TU, UK, psrak@bristol.ac.uk, Tel + 44 117 928 8461.

Disclosure
The authors have nothing to disclose

Europe PMC Funders Author Manuscripts

Europe PMC Funders Author Manuscripts

Introduction

Brain development is an ongoing process through fetal development and infancy. Normal migration, myelination, synaptogenesis and pruning are crucial for long term function. It is well known that pre-term birth is associated with cognitive, behavioural and motor differences throughout life.1–4 Typically, those born pre-term have lower cognitive performance relative to those born at-term. A major development process in the infant brain is myelogenesis, an important part of white matter (WM) development, whose purpose is to yield a huge increase in conduction speed along axons. Myelination does not occur for all the brain at once, but follows a general caudo-rostral gradient. For this reason, premature birth will “interrupt” the normal scheme of myelogenesis differently depending on gestational age (GA). Myelination subgroups have been defined according to whether myelination is detectable at term birth or not (groups A and B, respectively), and the subsequent rate of myelogenesis (groups A1-4, B1-4, 1=fastest).5 Generally, proximal pathways are myelinated earlier and faster than distal ones; sensory pathways earlier and faster than motor pathways; projection fibres earlier and faster than association fibres; central regions earlier and faster than polar/cortico-cortico regions.

MRI is a highly sensitive technique for monitoring brain maturation including WM microstructure and myelination. It is commonplace to report on the presence or number of “localised WM abnormalities” or diffuse excessive high signal intensity (DEHSI) on T2-weighted images, although these qualitative markers have limited prognostic value for clinical outcomes.6 Quantitative MRI7 by means of diffusion imaging and relaxometric imaging (T1 and T2 mapping) are particularly powerful modalities in the study of the developing brain, including myelogenesis. This is owing to the fact that water diffusion and relaxation are sensitive to the presence of microstructure on a cellular scale influencing the motion of water of which the developing myelin sheath is an important example. During fetal brain development, myelogenesis imposes a rapidly changing microstructural environment, which therefore confers great sensitivity to diffusion and relaxometric imaging.8

Diffusion tensor imaging (DTI) has been applied in studies of the developing brain, with the consistent result that diffusivities reduce rapidly, and fractional anisotropy (FA) increases rapidly, with GA across WM, though the rate and marginal mean is regionally dependent.9, 10 Decreasing radial diffusivity (RD) and increasing FA are reflective of the tortuosity imposed on water motion by the myelin sheath. Axial diffusivity (AxD) generally remains higher, decreasing more slowly. It is accepted that these processes are driven mainly by the development of restrictions to water motion (mainly the myelin sheath),11 rather than the total amount of water present, though the water content also decreases during myelogenesis. It is also known that T2 drops with GA12, and that T2 is a correlate of the qualitative DEHSI radiological marker.13

The prediction of clinical outcome from quantitative DTI indices obtained at term-equivalent age shows promise.14–17 Various studies have demonstrated that FA is lower and mean diffusivity (MD) higher at term-equivalent age in pre-term infants,18–21 and that measurements correlate with various future outcomes including visual performance,22

Europe PMC Funders Author Manuscripts

motor development,23, 24 and CP risk.25 The effect of pre-mature birth on DTI scalars at term-equivalent age has the implication of different patterns of WM development in accordance with time of birth.

Recent research has also begun to explore the utility of T2 relaxometry as a quantitative marker. A structural connectivity approach has shown that T2 is altered in infants born pre-term in certain cortical networks, but no association between T2 and GA was found.26 A combination of DTI and T2 data has also been used to demonstrate widespread retarded WM maturation as well as characterise the region-specific gestational age at which premature birth loses association with altered maturation.27 It was found that the critical GA for altered WM maturation followed a similar regional distribution to myelogenesis itself, centre-out and bottom-to-top.

We hypothesised that combining quantitative T2 data with DTI indices would enhance the specific detection of WM changes in two groups of infants (very preterm (VP), born before 32 weeks and late preterm (LP) born between 33 and 36 weeks) participating in MRI studies of infants at increased risk of neurodevelopmental abnormalities. We hypothesised that infants scanned at the same gestation (or postconceptual age) would show distinct differences in their patterns of WM development as a function of GA. Using a multivariate method we obtain a basis of variables which best discriminate the two groups, with the overall result that VP birth results in a retarded maturation of earlier-myelinating WM selectively. We also demonstrate that T2 is anisotropic in the infant brain, depending on the fibre-to-field angle.

Methods

Cohort

Infant data was analysed from subsets of two separately recruited cohorts at increased risk of adverse neurodevelopmental outcomes, both from studies carried out at St Michael's Hospital and the University of Bristol. 11 data sets came from a study of very and extreme preterm infants (Table 1). 28 This study had National Research Ethics approval (10/GO106/10) on behalf of the NHS Health Research Authority. 20 data sets came from a study of monochorionic diamniotic (MCDA) twins (Table 1). This study had National Research Ethics approval (15/SW/0230). All parents gave written informed consent for their children to participate in this study. The project was carried out in accordance with the Declaration of Helsinki.

MRI scanning

For DTI, images were acquired with the following parameters: 40 slices, 2 mm; TR = 9000ms; TE = 87ms; FOV = 200 mm; diffusion MDDW 30 directions. For T2 relaxometry, turbo spin echo (TSE) images were acquired with the following parameters: 20 slices, 4 mm; TR = 9000ms; three TE = 11ms/155ms/299ms; Flip 180°; FOV = 160 mm

All infants were scanned in natural sleep, without sedation. Prior to scanning, they were fed and settled to sleep. To minimise acoustic noise, we utilised mouldable putty (Affinis, Coltene, Switzerland) in the external auditory canal, and covered the ears with ear muffs

Europe PMC Funders Author Manuscripts

(Nautus, Seattle, WA, noise reduction of 7 dB). Infants were placed in a custom-made vacuum moulding cushion, which reduced movement and vibration, and may have made infants feel more secure. MRI compatible physiological monitoring equipment (In vivo Expression, Gainesville, FL) was used to monitor ECG and oxygen saturation. Infants were monitored during scanning for movement, or becoming unsettled.

Data analysis

Diffusion-weighted images were corrected for motion using EDDY_CORRECT command, and diffusion tensor images fitted using DTIFIT, assuming a single effective diffusion tensor for each voxel. T2 maps were fitted by assuming mono-exponential decay of signal intensity, and apply linear least squares in a logarithmic space. Tract-based spatial statistics (TBSS) was applied to analyse DTI scalars and T2 maps in WM. A processing pipeline was adapted from FSL, which we modified to make use of the JHU-Neonate template brain super-sampled to 0.6 mm isotropic resolution (FSL by default uses an adult FA map at 1 mm resolution). The FA threshold for skeletonisation was set at 0.175 to generate a WM skeleton mask. T2 maps were registered to the native DTI space using FNIRT, with the sum-over-echoes T2-weighted image from the TSE being registered to the B-value = 0 T2*-weighted image from the diffusion-weighted series (the contrast being similar and signal-to-noise ratio high). Like the RD, MD and AxD, T2 maps were fed into the TBSS pipepline using the TBSS_NON_FA, modified to take account of the altered template space.

Since the periods of gestation in the two groups were different, GA was not modelled as a linear confound, but a simple categorical variable of “group” was used. Similar analyses were performed comparing pre-term singletons to the lighter and heavier twin sub-groups separately, with similar results (not shown). Group differences were tested for by t-testing and 500 permutation tests. Threshold-free cluster enhancement was applied. Atlas-based analysis of the TBSS-derived WM skeleton was performed using the JHU-Neonate WM atlas.29

Based on permutation testing, we defined a “TBSS-positive” ROI to include any voxel in which any DTI scalar or T2 showed a significant difference between groups. To further elucidate the extent to which different quantities differ between groups, median values in all WM tracts of the JHU-Neonate WM atlas were calculated, masked by the TBSS-positive ROI. This dataset therefore contained median values of FA, RD, AxD and T2 for all 15 WM tracts in the TBSS-positive ROI (60 variables) for all 11 pre-term singletons and 20 twin infants. Principal component analysis (PCA)30 was first used to reduce the dimensionality of this 60-dimensional space to a 2-dimensional space. Linear discriminant analysis was then applied to seek a hyperplane best distinguishing the pre-term singletons from twins in the 2-dimensional reduced principal component basis. The “most significant” contributors to distinguishing groups from amongst the original basis of variables could then be identified by their projections onto the group-separating linear discriminant analysis (LDA) hyperplane. Such an approach has the advantage of effectively combining the statistical power of all 60 variables into only 2 dimensions.

Statistical analysis was performed using Matlab, Statistics and Machine Learning Toolbox v11.0 (Mathworks, Natick, MA).

Anisotropy of T2 was analysed in the DTI native space, supersampled to 1 mm isotropic resolution.31 Two sub-groups were defined: a VP and a LP group. Data in each sub-group were pooled. The computation of T2 anisotropy involves determining whether the angle between a main axis of order and the applied magnetic field (B0) has an effect on T2. The angle between the principal eigenvector of the diffusion tensor and B0 serves as a good experimental measure. The "extent" of order also has a large effect on anisotropy of T2, FA is used as an experimental measure of "extent of order". Therefore, for each 2D bin-range of fibre-to-field angle and FA, all T2 observations across the sub-group are averaged. A surface plot can then be assembled. To the surface plot, we fit the model30 recently derived:

$$T_2 = \frac{T_2^{iso}}{1 + T_2^{iso} A \sin^4 \theta_{FB}} \quad \text{Eq.1}$$

Where T_2^{iso} is the isotropic or parallel-to-field T2, A is the amplitude of anisotropy and theta is the fibre-to-field angle.32 This is fitted for each FA bin-centre separately to generate its parameters as a function of FA.

Results

Relationship between T2 and DTI scalars

Boxplots of T2 and DTI scalars across the entire cohort for each WM tract of the JHU-Neonate atlas are shown (Figure 1). These plots are all sorted by descending FA within each myelogenesis subgroup. There is a clear trend towards longer T2 and higher diffusivities (MD, RD, AxD) in late-myelinating WM. FA shows a weaker effect of myelogenesis group, though we must keep in mind that the boxplots absorb the variance caused by effects of participant group and individual factors. In the SI T2 is strongly correlated with DTI scalars, and most strongly with RD (R = 0.9189), a point we return to later.

Inter-group differences

Differences between the term-equivalent DTI scalars and T2 maps of infants either in the VP or LP groups were assessed on a voxel-wise basis by t- and permutation testing, based on the TBSS-derived WM skeleton mask. This identified extensive regions in which T2 and DTI scalars differed between groups (Figures 2-3). As there was the possibility that discordant blood supply to different twins in each MCDA pair in the LP group could impact on WM development, we specifically compared the higher and lower birthweight twin from each pair (using weight as a surrogate marker of proportional in utero blood supply). As we did not detect differences between 'heavier' and 'lighter' twins, we increased our power by collectively analysing their data as a single (LP) group. The group-separating potential was concentrated more in the earlier-myelinating WM, with the exception of the MCP which showed no difference in any parameter (Figure 3).

We also found that there remained an effect of participant group (VP vs LP), but only on FA and T2, if GA was modelled as a linear confound effect (not shown). That is, T2 and FA are different between VP singletons and LP twins due to effects of both GA and some other

discriminating factor between participant group, whereas MD, AxD and RD differ only due to the effect of GA (for it can be regressed out). Possibilities include a specific effect of being a multiple birth, or of chorionicity. Alternatively, there may be a non-linear effect of GA on FA and T2, although data argue for a linear effect (not shown). A possibility is that an unknown factor non-linearly correlated with GA, such as requirement for mechanical ventilation or other intensive care intervention has a discriminative effect on FA and T2, but not RD or MD.

The results of combining the tract-wise (term-equivalent) T2, FA, RD and AxD tract-wise TBSS-positive medians to determine the most significant contributions to distinguishing VP infants from LP twins are shown (Figure 4). We defined simple criteria to select the largest contributors to separating groups, namely those variables whose projection onto an axis normal to the LDA hyperplane was > 0.15. This implies that we define as the “largest contributors to separating groups” those variables for which more than 15% variance is accounted for by group. The FA of nearly all tracts contributed to overall group separation. The T2 of most group-A tracts contributed (except the MCP), as well as the entire corpus callosum and uncinated fasciculus, but no tracts from group B3. From AxD, ar (group A) and cg (B2) contributed only. RD did not contribute at all. Overall, then, FA is generally most different at term-equivalent age between VP and LP groups, with T2 also being discriminatory.

Receiver operating characteristics (ROC) curves and statistics showed an area-under-curve (AUC) of 0.964, false positive rate (FPR) of 0.050, and true positive rate (TPR) of 0.818. K-fold cross-validation was performed, revealing class loss of 0.1619. If T2 was not included, the AUC was 0.9545, FPR 0.150, TPR 1.000, but class loss 0.2581.

Anisotropy of T2

Anisotropy of T2 was assessed in the VP and LP sub-groups. Fitted T2 surfaces as a function of fibre-to-field angle and FA, across all WM are shown (Figure 5). As in previously published work on the adult brain,31, 33 T2 is longest when parallel to B0.31, 33 This effect is smaller at lower FA, such that T2 anisotropy occurs only where there is considerable order. At higher FA values, the peak-to-trough T2 is up to ~20 ms in the pre-term group but only 10 ms in the LP group. Although peak-to-trough distances are similar to the adult brain, the amplitudes of anisotropy are about 10-fold lower31 (and FA two to four-fold). Surprisingly, the amplitude of anisotropy is largest in the VP group for any given FA.

Discussion

We have explored the relationships between DTI scalars and quantitative T2 in WM, at term-equivalent age, of VP infants born before 32 weeks completed GA and MCDA twins born after 33 weeks. We have shown that T2 relaxation time at term-equivalent age, as well as DTI scalars, show wide-spread differences according to GA. We have also demonstrated that T2 is anisotropic in the infant brain, having an orientation dependence on fibre-to-field angle, and that this dependence is different between VP and LP infants.

We observed, in general, markers of “less developed” WM in the VP group, with FA and T2 having the largest effects, and with a strong bias towards earlier-myelinating WM. By modelling the effect of GA as linear, we conclude that this difference is dominated by an effect of GA, but that there is a more limited effect of participant group. The changes in WM microstructure probed by T2 and DTI scalars in the developing brain are dominated by myelogenesis, such that one can expect the group differences to reflect different myelogenesis pathways according to GA group. The VP group appears to show a myelogenesis pathway that is generally lagging behind the LP group at term-equivalent age, with the early-myelinating regions suffering the greatest adverse effects. Late-myelinating regions, inasmuch as not showing an effect of GA up to the detection limit of our experiment (as a continuous variable or categorical group variable), arguably follow a more similar myelogenesis pathway, being less affected by premature birth. It is also possible that late-myelinating regions also follow a different myelogenesis pathway according to GA, but that such a difference becomes apparent at a later life. Group B tracts are not substantially myelinated at 40 weeks gestation, so such a difference may not be within the detection limit of our experiment.

The observation that DTI indices obtained at term-equivalent age imply retarded WM maturation in pre-term infants has been made in other studies.9, 10 Many have focused on selected WM regions, often the PLIC, CST or CC (see Table 2). However, there have been limited efforts to combine T2, in particular so the anisotropy of T2, with DTI, across an entire WM atlas, to build a high statistical power classifier for prematurity. In doing so, we have shown that combining sources of information from T2 and DTI across WM can classify the “state” of WM at term-equivalent age with impressive sensitivity and specificity. These data argue for incorporating use of T2 relaxometry in assessing whether the state of the brain differs from expectation as a result of pre-term birth.

The inter-group differences observed for T2, as well as effect sizes for GA, were larger and more widespread than in recent work using T2 and DTI in concert.27 Broadly, however, our work using both T2 and DTI, with a multivariate analysis to combine statistical power, agrees with recent findings that earlier GA is associated with markers of retarded WM maturation, in particular in earlier-myelinating regions.10 Our limitation to a TBSS-derived WM skeleton and use of dimensionality reduction and machine learning may explain our increased statistical power, as well as instrumental differences.

We found that T2 is anisotropic in the infant brain at term-equivalent age, with amplitude in WM that is approximately $1/10^{th}$ of that reported in adults.31 The lower anisotropy implies a more homogeneous magnetic field on a mesoscopic scale, from which we may infer a lower susceptibility difference between axon walls and their surroundings. This implies less, or less ordered, myelin within the developing myelin sheaths. The higher isotropic part of T2 in infants relative to adults probably reflects higher overall water content in infants.

Recent work has shown that T2 and diffusion anisotropy34 are coupled phenomena,34 so this observation is at first curious given that our results mainly argue for retarded WM maturation in infants born at an earlier GA. Anisotropy of T2 is, according to theory, caused by radial diffusion through anisotropic magnetic fields created by the myelin sheath and/or

other ordered structures with different magnetic properties from water. The fact that the T2 anisotropy is driven by radial diffusion means that the results are not at odds with the findings for FA and AxD (which report different phenomena). In consideration that the RD is better correlated with T2 than any other DTI scalar, this result is self-consistent.

The question remains as to how T2 anisotropy may differ without any other parameter changing, and what this tells about WM. T2 and DTI are more sensitive to intracellular and interstitial water, diffusion of molecules in the myelin sheath is not directly seen due to fast relaxation. Nonetheless, the susceptibility difference between water and the accumulating myelin drives the T2 anisotropy, such that we need not see DTI changes even if the myelin sheaths differ in structure and molecular composition between groups. Inter-group T2 anisotropy differences may therefore reflect a differently structured myelin sheath, or an altered molecular composition which alters its magnetic susceptibility. This may give T2 anisotropy the capability to detect differences in molecular composition of the myelin sheath, rather than structural changes, which may also account for the improved group discriminating power upon inclusion of T2.

Our study has some limitations. Firstly, T2 measurements are based on a simple mono-exponential approximation to a 3-echo TSE. In reality, at short echo times, decoherence is more rapid than a mono-exponential model can explain, and is usually attributed to the pool of water associated with the myelin sheath itself – vindicated by the observation that decoherence loses its early fast-decay behaviour in non-myelinating axons.35 This pool is essentially invisible to our experiments (including DTI) directly, though the effects are manifest indirectly (through exchange, tortuosity and susceptibility-driven T2 anisotropy). A prohibitively lengthy T2 mapping sequence may be needed to sample early and late decoherence sufficiently to generate high-quality non-exponential or multi-exponential T2 maps.

Secondly, we limited our analysis to a TBSS-derived symmetrised WM skeleton. Therefore, we neglect cortical and subcortical GM. However, the difficulties in segmenting tissue classes in our cohort are such that we would run the risk of including misclassified tissue. Low anatomical resolution also confounds analysis of cortical regions. Symmetrisation is argued for by being blind to the handedness of the participants (which is developed only at a later age). We lose specificity (right vs left), but it is unlikely that the overall sensitivity of our experiment to characterise the effects of prematurity on development pathways is compromised.

Thirdly, GA is not the only independent variable differing between the groups, as the LP group contained entirely twins and the VP group were mainly singleton. Whilst the differences in anisotropy which are linearly associated with GA are clearly interpretable, there are other differences which could reflect a number of potential between-group differences. However, this confound of multiple group differences does not alter the observation that combined FA and T2 anisotropy measures provide a clear means of differentiating states of WM maturation in neonates independent of cause. Future work examining the relationship of WM maturation at term-equivalent age with long term neurodevelopmental outcome is warranted to determine whether this multimodal

Europe PMC Funders Author Manuscripts

quantitative mapping can improve prognostic specificity and aid clinical decisions for infants at increased risk of abnormal development.

To conclude, we propose that the characterisation of WM development in pre-term infants may benefit form a combined T2 relaxometry/DTI approach. Our data indicate that VP infants show widespread retarded WM maturation at term-equivalent age, which a combination of T2 mapping and DTI can quantify with high sensitivity and specificity. Additional work will be needed to determine to what extent this is predictive of future treatment need, and how to best use this powerful information to bring about the best patient outcome.

Acknowledgements

MJK is funded by the Elizabeth Blackwell Institute and by the Wellcome Trust international strategic support fund [ISSF2: 105612/Z/14/Z]. The work received support from the Dunhill Medical Trust [grant number R385/1114].

References

1. Bhutta AT, Cleves MA, Casey PH, Cradock MM, Anand KJ. Cognitive and behavioral outcomes of school-aged children who were born preterm: a meta-analysis. JAMA. 2002; 288:728–7. [PubMed: 12169077]
2. de Kieviet JF, Piek JP, Aarnoudse-Moens CS, Oosterlaan J. Motor development in very preterm and very low-birth-weight children from birth to adolescence: A meta-analysis. JAMA. 2009; 302:2235–42. [PubMed: 19934425]
3. Marlow N, Hennessy EM, Bracewell MA, Wolke D. Motor and executive function at 6 years of age after extremely preterm birth. Pediatrics. 2007; 120:793–804. [PubMed: 17908767]
4. Johnson S, Hennessy E, Smith R, et al. Academic attainment and special educational needs in extremely preterm children at 11 years of age: the EPICure study. Arch Dis Child Fetal Neonatal Ed. 2009; 94:F283–9. [PubMed: 19282336]
5. Kinney HC, Brody BA, Kloman AS, Gilles FH. Sequence of central nervous system myelination in human infancy. II. Patterns of myelination in autopsied infants. J Neuropathol Exp Neurol. 1988; 47:217–34. [PubMed: 3367155]
6. Van't Hooft J, van der Lee JH, Opmeer BC, et al. Predicting developmental outcomes in premature infants by term equivalent MRI: systematic review and meta-analysis. Syst Rev. 2015; 4:71. [PubMed: 25982565]
7. Tofts, P. Quantitative MRI of the Brain: Measuring Changes Caused by Disease. Chichester, England: John Wiley& Sons, Ltd; 2004.
8. Dubois J, Dehaene-Lambertz G, Kulikova S, et al. The early development of brain white matter: A review of imaging studies in fetuses, newborns and infants. Neuroscience. 2014; 276:48–71. [PubMed: 24378955]
9. Pieterman K, Plaisier A, Govaert P, et al. Data quality in diffusion tensor imaging studies of the preterm brain: a systematic review. Pediatr Radiol. 2015; 45:1372–81. [PubMed: 25820411]
10. Partridge SC, Mukherjee P, Henry RG, et al. Diffusion tensor imaging: serial quantitation of white matter tract maturity in premature newborns. Neuroimage. 2004; 22:1302–14. [PubMed: 15219602]
11. Beaulieu C. The basis of anisotropic water diffusion in the nervous system – a technical review. NMR Biomed. 2002; 15:435–55. [PubMed: 12489094]
12. Counsell SJ, Kennea NL, Herlihy AH, et al. T2 relaxation values in the developing preterm brain. AJNR Am J Neuroradiol. 2003; 24:1654–60. [PubMed: 13679288]
13. Hagmann CF, De Vita E, Bainbridge A, et al. T2 at MR imaging is an objective quantitative measure of cerebral white matter signal intensity abnormality in preterm infants at term-equivalent age. Radiology. 2009; 252:209–17. [PubMed: 19561257]

14. Pannek K, Scheck SM, Colditz PB, Boyd RN, Rose SE. Magnetic resonance diffusion tractography of the preterm infant brain: a systematic review. Dev Med Child Neurol. 2014; 56:113–24. [PubMed: 24102176]
15. Li K, Sun Z, Han Y, et al. Fractional anisotropy alterations in individuals born preterm: a diffusion tensor imaging meta-analysis. Dev Med Child Neurol. 2015; 57:328–38. [PubMed: 25358534]
16. Jaspers E, Byblow WD, Feys H, Wenderoth N. The corticospinal tract: A biomarker to categorize upper limb functional potential in unilateral cerebral palsy. Front Pediatr. 2015; 3:112. [PubMed: 26779464]
17. Plaisier A, Govaert P, Lequin MH, Dudink J. Optimal timing of cerebral MRI in preterm infants to predict long-term neurodevelopmental outcome: a systematic review. AJNR Am J Neuroradiol. 2014; 35:841–7. [PubMed: 23639558]
18. van Pul C, van Kooij BJ, de Vries LS, et al. Quantitative fiber tracking in the corpus callosum and internal capsule reveals microstructural abnormalities in preterm infants at term-equivalent age. AJNR Am J Neuroradiol. 2012; 33:678–84. [PubMed: 22194382]
19. Hasegawa T, Yamada K, Morimoto M, et al. Development of corpus callosum in preterm infants is affected by the prematurity: in vivo assessment of diffusion tensor imaging at term-equivalent age. Pediatr Res. 2011; 69:249–54. [PubMed: 21131895]
20. Thompson DK, Inder TE, Faggian N, et al. Characterization of the corpus callosum in very preterm and full-term infants utilizing MRI. Neuroimage. 2011; 55:479–90. [PubMed: 21168519]
21. Rose J, Vassar R, Cahill-Rowley K, et al. Brain microstructural development at near-term age in very-low-birth-weight preterm infants: an atlas-based diffusion imaging study. Neuroimage. 2014; 86:244–56. [PubMed: 24091089]
22. Bassi L, Ricci D, Volzone A, et al. Probabilistic diffusion tractography of the optic radiations and visual function in preterm infants at term equivalent age. Brain. 2008; 131:573–82. [PubMed: 18222994]
23. Krishnan ML, Dyet LE, Boardman JP, et al. Relationship between white matter apparent diffusion coefficients in preterm infants at term-equivalent age and developmental outcome at 2 years. Pediatrics. 2007; 120:e604–9. [PubMed: 17698966]
24. De Bruine FT, Van Wezel-Meijler G, Leijser LM, et al. Tractography of white-matter tracts in very preterm infants: a 2-year follow-up study. Dev Med Child Neurol. 2013; 55:427–33. [PubMed: 23441853]
25. Kim DY, Park HK, Kim NS, Hwang SJ, Lee HJ. Neonatal diffusion tensor brain imaging predicts later motor outcome in preterm neonates with white matter abnormalities. Ital J Pediatr. 2016; 42:104. [PubMed: 27906083]
26. Pannek K, Hatzigeorgiou X, Colditz PB, Rose S. Assessment of structural connectivity in the preterm brain at term equivalent age using diffusion MRI and T2 relaxometry: a network-based analysis. PLoS One. 2013; 8:e68593. [PubMed: 23950872]
27. Wu D, Chang L, Akazawa K, et al. Mapping the critical gestational age at birth that alters brain development in preterm-born infants using multi-modal MRI. Neuroimage. 2017; 149:33–43. [PubMed: 28111189]
28. Inder TE, Wells SJ, Mogridge NB, Spencer C, Volpe JJ. Defining the nature of the cerebral abnormalities in the premature infant: a qualitative magnetic resonance imaging study. J Pediatr. 2003; 143:171–9. [PubMed: 12970628]
29. Oishi K, Mori S, Donohue PK, et al. Multi-contrast human neonatal brain atlas: application to normal neonate development analysis. Neuroimage. 2011; 56:8–20. [PubMed: 21276861]
30. Levman J, Takahashi E. Multivariate analyses applied to healthy neurodevelopment in fetal, neonatal, and pediatric MRI. Front Neuroanat. 2015; 9:163. [PubMed: 26834576]
31. Knight MJ, Dillon S, Jarutyte L, Kauppinen RA. Magnetic resonance relaxation anisotropy: Physical principles and uses in microstructure imaging. Biophys J. 2017; 112:1517–28. [PubMed: 28402893]
32. Biagi L, Abbruzzese A, Bianchi MC, et al. Age dependence of cerebral perfusion assessed by magnetic resonance continuous arterial spin labeling. J Magn Reson Imaging. 2007; 25:696–702. [PubMed: 17279531]

33. Knight MJ, Wood B, Coulthard E, Kauppinen RA. Anisotropy of spin-echo T2 relaxation by magnetic resonance imaging in the human brain in vivo. Biomed Spectr Imag. 2015; 4:299–310.
34. Knight MJ, Kauppinen RA. Diffusion-mediated nuclear spin phase decoherence in cylindrically porous materials. J Magn Reson. 2016; 269:1–12. [PubMed: 27208416]
35. Beaulieu C, Fenrich FR, Allen PS. Multicomponent water proton transverse relaxation and T2-discriminated water diffusion in myelinated and nonmyelinated nerve. Magn Reson Imaging. 1998; 16:1201–10. [PubMed: 9858277]

Europe PMC Funders Author Manuscripts

Europe PMC Funders Author Manuscripts

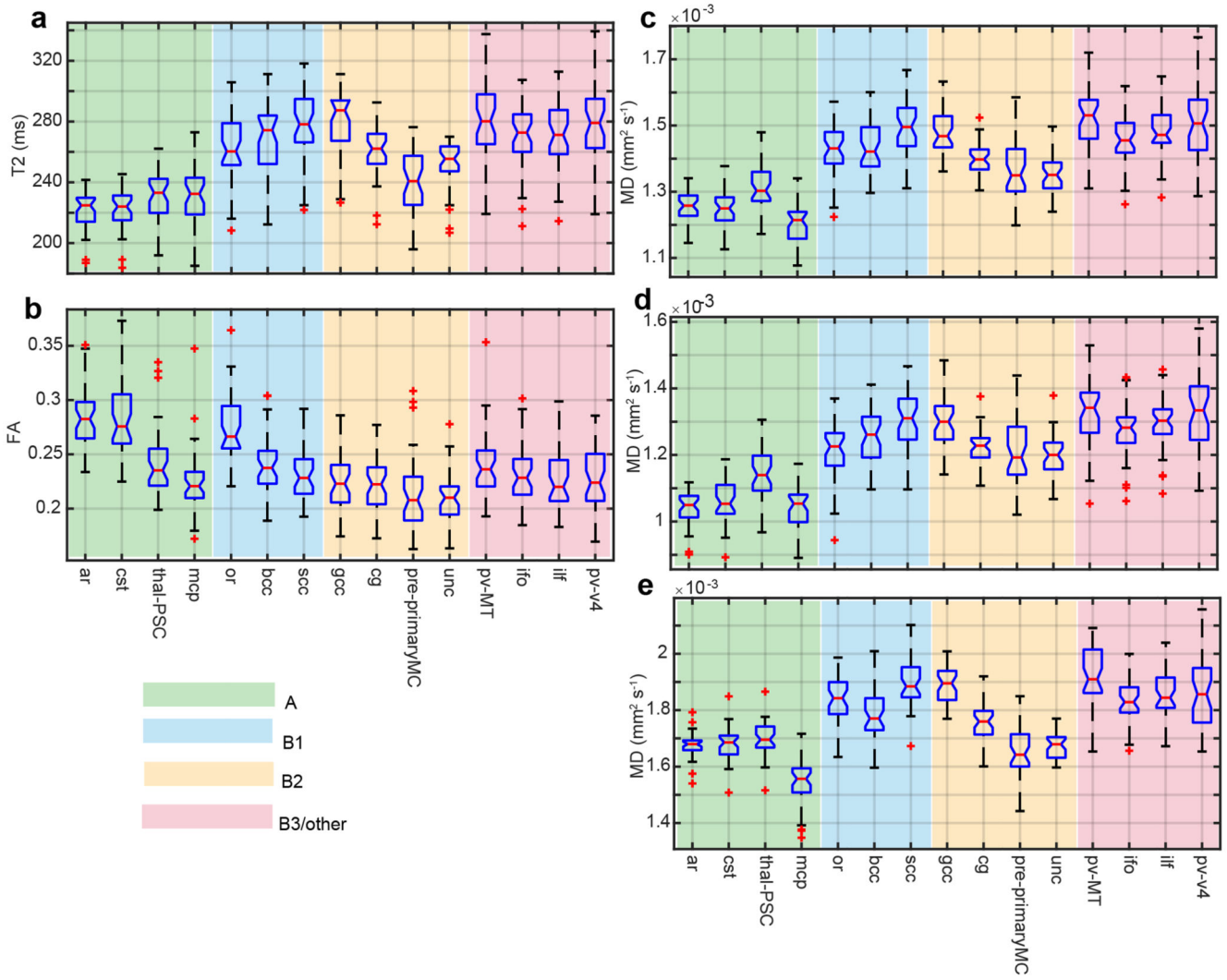

Figure 1.

Boxplots of TBSS-derived medians for DTI scalars and T2 across the whole cohort. The graphs are sorted by descending FA within each myelogenesis group (indicated by color) are as follows: A = myelination detectable at term age; B1 = no myelination detectable at term age, fast rate of myelination after birth; B2 = no myelination detectable at term age, intermediate rate of myelination after birth; B3/other = no myelination detectable at term age, slow rate of myelination after birth. Abbreviations used: FA = fractional anisotropy; MD = mead diffusivity. See Table 2 for white matter tract abbreviations.

Europe PMC Funders Author Manuscripts

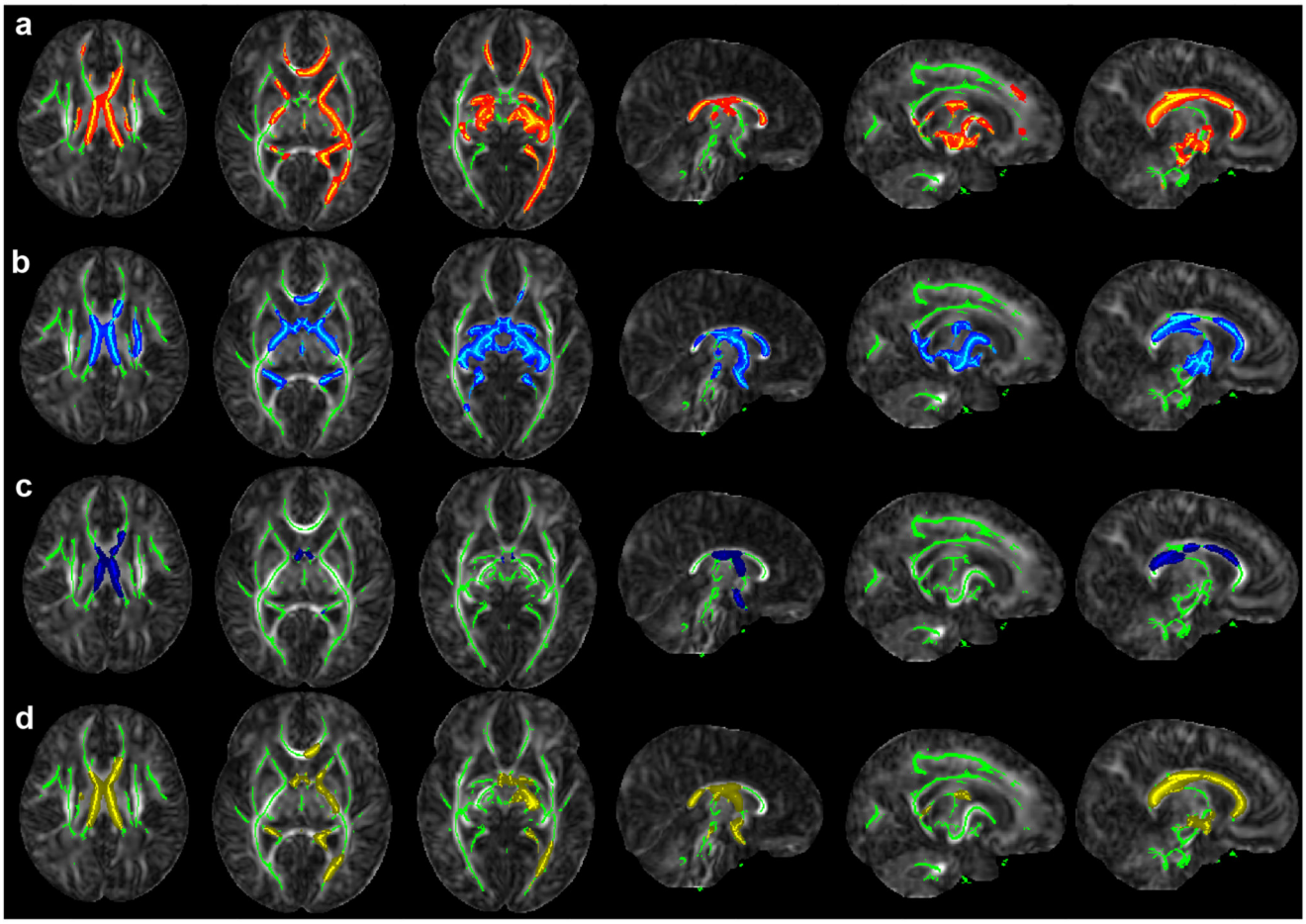

Figure 2.

Clusters in which VP infants differ from LP MCDA twins.

Row a: FA(VP) < FA(LP), Row b: T2(VP) > FA(LP), Row c: MD(VP) > MD(LP), Panel 3: RD(VP) > RD(LP). VP = very pre-term, LP = late pre-term MCDA twins. Colored voxels belong to clusters identified using threshold-free cluster enhancement at the $p < 0.05$ level using 500 permutations. Green marks the TBSS-demarcated WM skeleton. Results are shown on the JHU-Neonate FA template. Abbreviations used: MCDA = monochorionic diamniotic twin; MD = mean diffusivity; RD = radial diffusivity; WM = white matter; FA = fractional anisotropy.

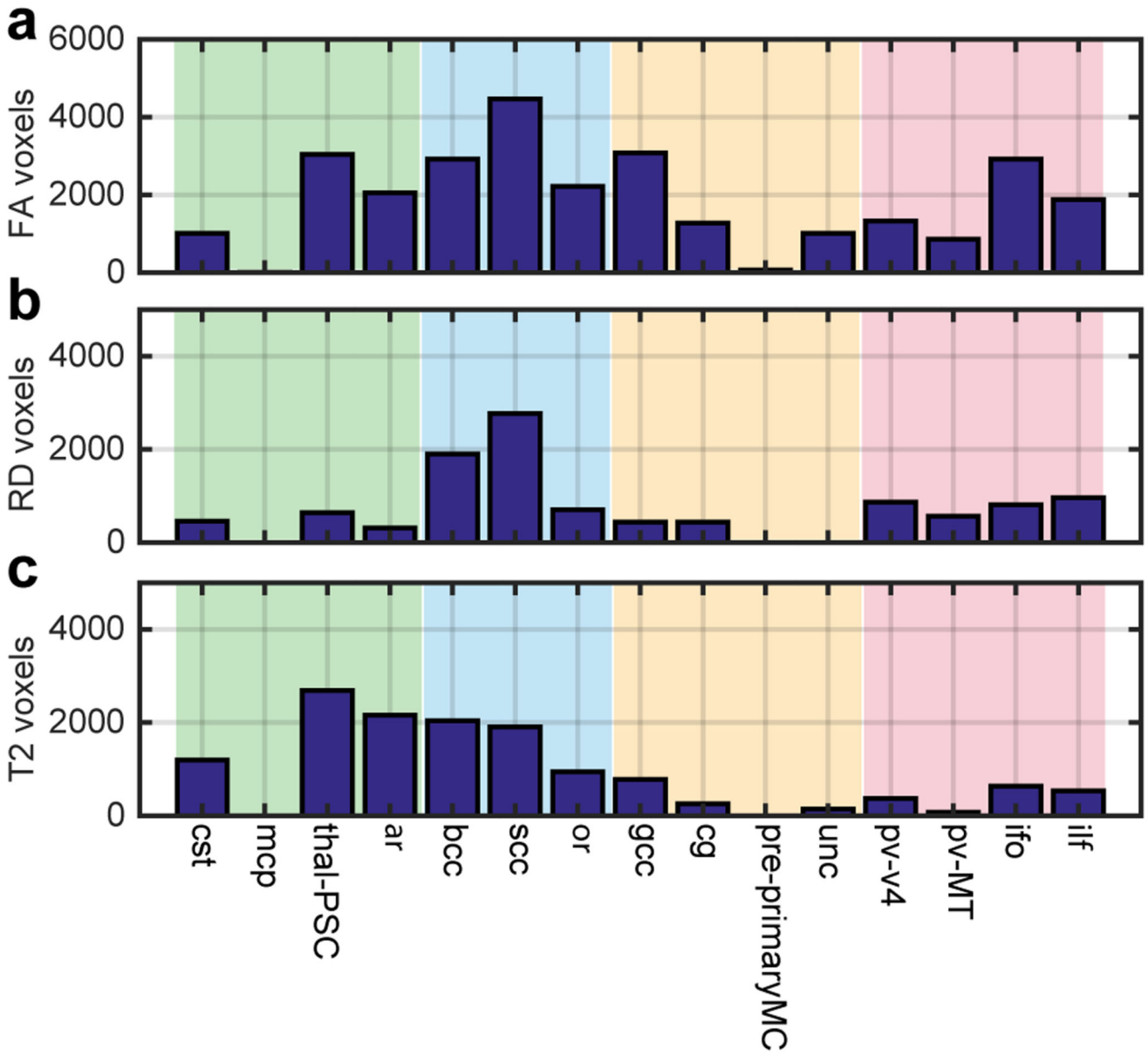

Figure 3.

Number of voxels in each WM tract separating the VP from LP groups at term-equivalent age.

Abbreviations used: VP = very preterm; LP = late preterm; WM = white matter; RD = radial diffusivity; FA = fractional anisotropy. See Table 2 for WM tract abbreviations

Europe PMC Funders Author Manuscripts

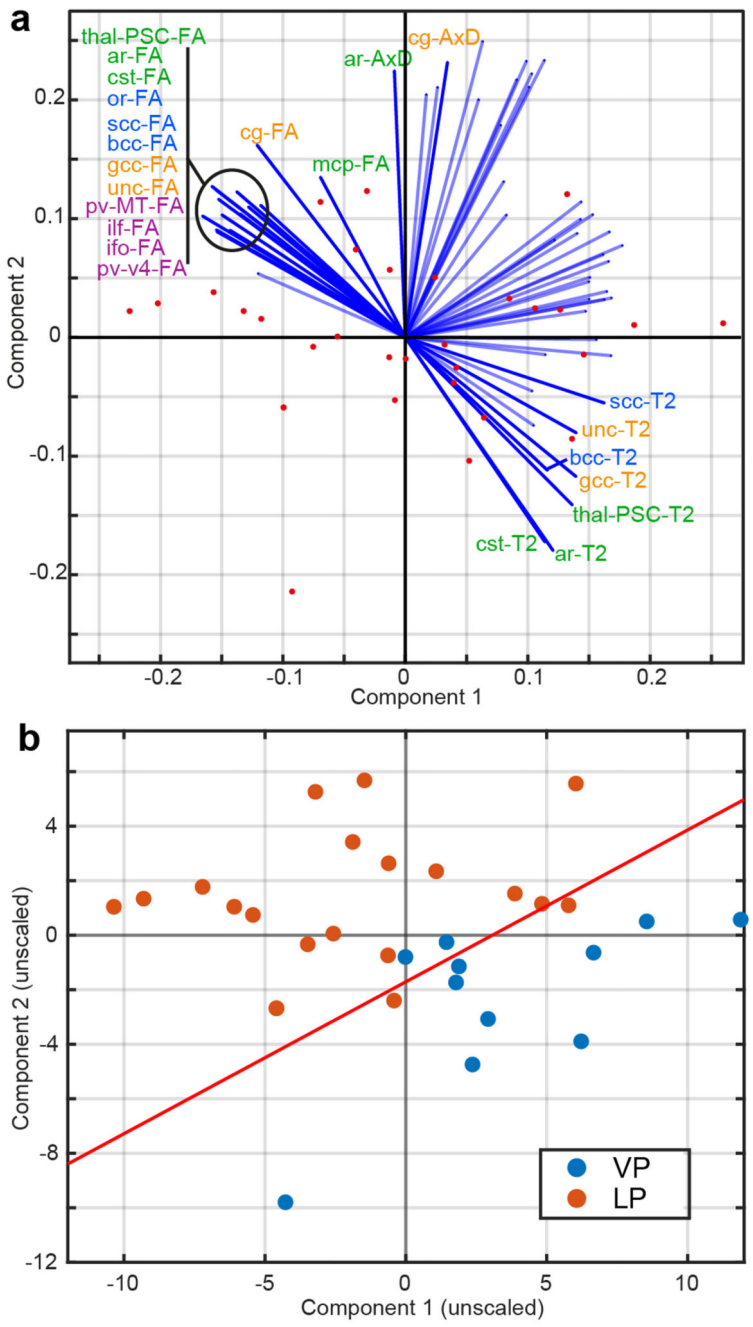

Figure 4.

PCA and LDA of tract-wise median DTI scalars and T2 in the TBSS-positive ROI. Panel a shows PCA, reduced to 2 dimensions, with the original variables labelled as projections. The projections are labelled (and in solid color) if their projection normal to the LDA hyperplane is > 0.15, which implies that more than 15% of the variance in that variable is accounted for by group. Text labels are colored by myelogenesis group. Panel b shows the PCA with data points labelled by group, as well as the LDA hyperplane as a solid line. Abbreviations used:

PCA = principal component analysis; LDA = linear discriminant analysis; VP = very preterm; LP = late preterm. See Table 2 for WM tract abbreviations.

Europe PMC Funders Author Manuscripts

Europe PMC Funders Author Manuscripts

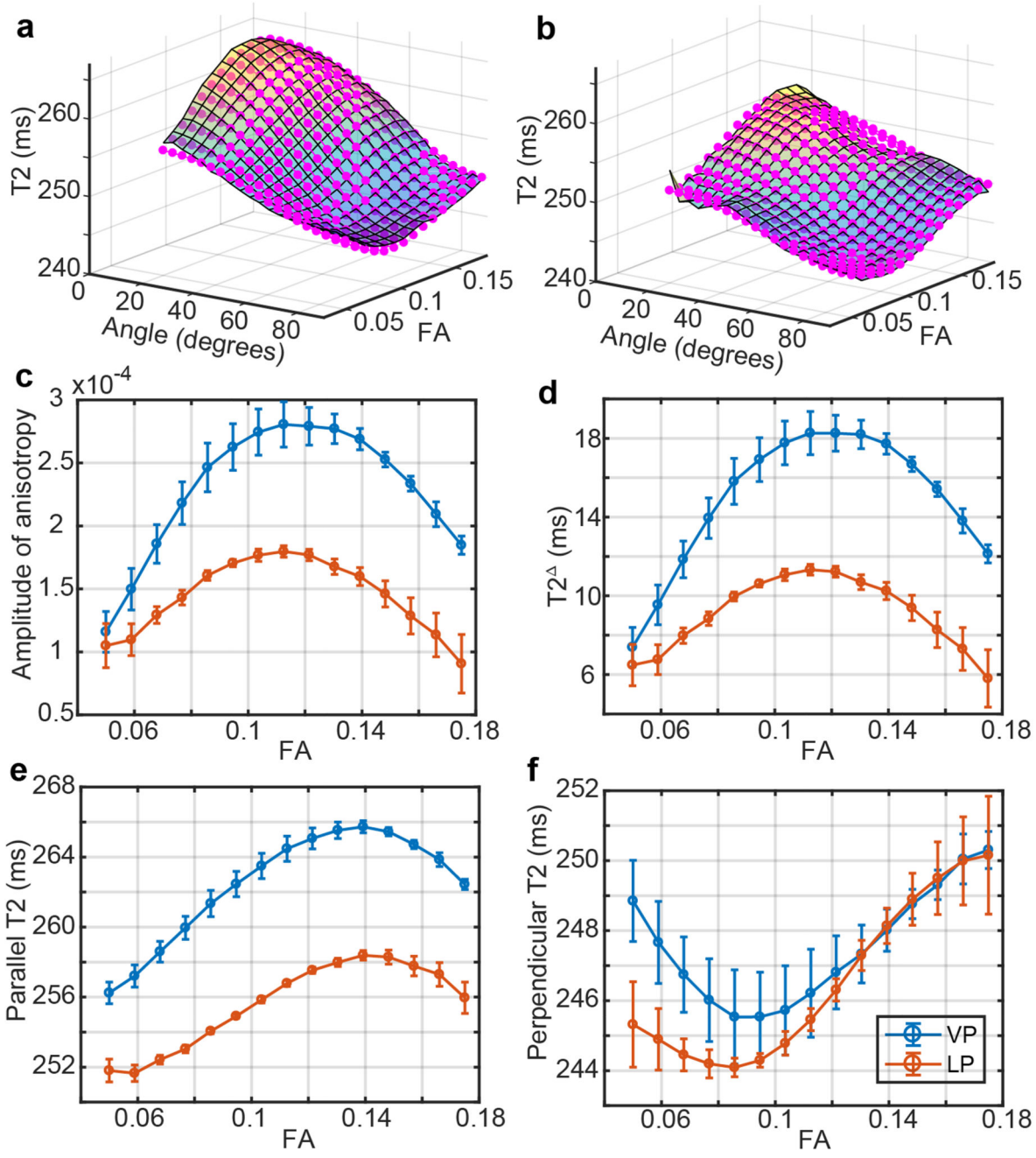

Figure 5.

T2 anisotropy in the term-equivalent infant brain. Panels a and b show surfaces of T2 against FA and the fibre-to-field angle obtained from DTI, with each plotted value of the opaque surface being the average value in the corresponding 2D bin range. Magenta points are the fit of Eq. 1. The VP and LP groups are plotted in a and b respectively. Panels c-f show, respectively, the fitted values at each FA bin range of the amplitude of anisotropy A, $T2^{\Delta}$,

$T2^{||}$ and $T2^{per}$. Abbreviations used: VP = very preterm; LP = late preterm; FA = fractional anisotropy.

Europe PMC Funders Author Manuscripts

Europe PMC Funders Author Manuscripts

Table 1

Demographic and clinical characteristics of neonate groups.

Characteristics	Late preterm group	Very preterm group
Number of neonates	20	11
GA at birth	35w 4d (33w 5d – 36w 3d)	27w 3d (25w 2d – 31w 2d)
Median GA at MRI	38w 0d (37w 0d – 38w 5d)	37w 4d (37w 0d – 40w 6d)
Male gender	14	6
Multiple pregnancy	20	2
Antenatal steroids	12	9
Chorioamnionitis	2	3
Mechanical ventilation	2	10
Inotropic support	1	1
Normal clinical MRI	19	6
Mild WM abnormality	1	2
Moderate WM abnormality	0	1
Intraventricular hemorrhage	0	3

Gestational age given as median and range; WM abnormalities in clinical MR according to criteria given by Inder et al.28. Presence of intraventricular hemorrhage determined by MRI.

Europe PMC Funders Author Manuscripts

Table 2

Abbreviations used in text and Figures for WM tracts

Abbreviation	Whole name
ar	acoustic radiation
bcc	body of corpus callosum
cg	cingulum
cst	cortico-spinal tract
gcc	genu of corpus callosum
ifo	inferior fronto-occipital fasciculus
ilf	inferior longitudinal fasciculus
mcp	middle cerebral peduncle
or	optic radiatum
PLIC	posterior limb of internal capsule
pre-primaryMC	pre-primary motor cortex
pv-MT	primary visual middle temporal area (area 5)
pv-V4	primary visual area 4
scc	splenium of corpus callosum
thal-PSC	thalamic-primary somatosensory cortex
unc	uncus